

# Impact of OCT scan-patterns in identifying morphological features of lamellar macular holes and macular pseudoholes

Osman Murat Uyar<sup>1</sup>, Jonas Neubauer<sup>2</sup>, Francoise Sadler<sup>2</sup>, Eva-Maria Konrad<sup>2</sup>, Faik Gelisken<sup>2</sup>

<sup>1</sup>Department of Ophthalmology, Ulus Liv Hospital, Istanbul 34340, Turkey

<sup>2</sup>Department of Ophthalmology, Eberhard-Karls University, Tuebingen 72076, Germany

**Co-first authors:** Osman Murat Uyar and Jonas Neubauer

**Correspondence to:** Jonas Neubauer. Department of Ophthalmology, Eberhard-Karls University, Tuebingen 72076, Germany. StudyJN@Outlook.com

Received: 2021-11-24 Accepted: 2022-01-25

## Abstract

• **AIM:** To evaluate the impact of the optical coherence tomography (OCT) scan patterns on the detection of the features associated with lamellar macular hole (LMH) and macular pseudohole (MPH).

• **METHODS:** This is a retrospective analysis of 100 consecutive eyes with LMH ( $n=41$ ) and MPH ( $n=59$ ) having at least three of the following OCT features, which include mandatory criteria for the diagnosis of LMH and MPH: Epiretinal membrane, epiretinal proliferation, verticalization, intraretinal cystoid spaces, foveoschisis, irregular foveal contour, foveal cavity with undermined edges, and ellipsoid line disruption. Primary outcome measurement was the detection frequency of the features in three different OCT scan patterns: 1) volume scan; 2) six radial scans (R6); and 3) vertical and horizontal radial scans (R2).

• **RESULTS:** Of the total eight features, the maximal detection frequency was found as  $4.45 \pm 1.45$ ,  $4.35 \pm 1.47$ , and  $3.70 \pm 1.59$ , by the volume, R6 and R2, respectively. R2 was inferior to the other patterns in detection of the total features ( $P < 0.001$ ), whereas R6 and volume patterns were found comparable ( $P = 0.312$ ).

• **CONCLUSION:** The physician should be aware that the selection of the OCT-scan pattern may influence the detection of mandatory morphological criteria for the diagnosis of LMH and MPH.

• **KEYWORDS:** diagnosis; epiretinal membrane; lamellar macular hole; macular pseudohole; optical coherence tomography

**DOI:**10.18240/ijo.2022.07.08

**Citation:** Uyar OM, Neubauer J, Sadler F, Konrad EM, Gelisken F. Impact of OCT scan-patterns in identifying morphological features of lamellar macular holes and macular pseudoholes. *Int J Ophthalmol* 2022;15(7):1089-1094

## INTRODUCTION

The improvements of the optical coherence tomography (OCT) technique have enabled the investigators detailed morphological analysis of the vitreomacular interface diseases. Especially the OCT characteristics of the epiretinal membrane (ERM), lamellar macular hole (LMH) and macular pseudohole (MPH) have been reported frequently<sup>[1-6]</sup>. New concepts regarding the classification and nomenclature of the vitreomacular interface diseases are proposed<sup>[7-11]</sup>. Thus, LMH is characterised by the presence of irregular foveal contour, the presence of a foveal cavity with undermined edges and the apparent loss of foveal tissue<sup>[11]</sup>. MPH is defined by the presence of a foveal sparing ERM, a steepened foveal profile and an increased central retinal thickness<sup>[11]</sup>. Beside the visualisation and interpretation of the OCT-features, it became also evident, that the OCT-examination technique may have an influence on the detection of morphological features of the macula<sup>[12-13]</sup>.

The experienced retina specialists are using the appropriate OCT-scan pattern with high image quality. On the other hand, to our knowledge no evaluation of the OCT-scan patterns for the investigation of the OCT-features was performed in the specific field of LMH and MPH. The current evidence is only based on the anecdotal transfer of routine experience of the experts.

In the presented study, we evaluated the impact of different OCT scan patterns on the detection of morphological features seen in LMH and MPH.

## SUBJECTS AND METHODS

**Ethical Approval** Approval of the Institutional Ethic Committee of the University of Tuebingen was obtained before the analysis of the data (Project 685/2020BO). The study has been performed in accordance with the Declaration of Helsinki.

This is a retrospective analysis of 100 consecutive eyes (100 patients). Patients diagnosed as ERM, LMH or MPH from March 2017 to July 2019 in the Department of Ophthalmology

of the University Tuebingen were selected by screening of the digital chart archive. Inclusion criteria were the presence of at least three of the following OCT features: ERM, epiretinal proliferation, verticalization, intraretinal cystoid spaces, foveoschisis, irregular foveal contour, foveal cavity with undermined edges and ellipsoid line disruptions. Because of the low incidence of the pseudo-operculum in our cohort and possible intra- and interrater measurement differences of the central retinal thickness, these two features were not included into the analysis. Exclusion criteria were diseases affecting the posterior pole, such as advanced age-related macular degeneration, diabetic maculopathy, high myopia [ $>-6.0$  diopters (D)], choroidal neovascularization, retinal venous occlusions, uveitis, ocular trauma, retinal tear, previous intraocular surgery except for cataract extraction, retinal cryotherapy and laser photocoagulation. Eyes with ERM-only were also excluded. Forty-one eyes had LMH and 59 eyes had MPH. OCT was performed by the Spectralis OCT (Heidelberg Engineering GmbH, Heidelberg, Germany) and reviewed with the Heidelberg Eye Explorer (version 1.9.1.3.0) using the HRA/Spectralis Viewing Module (version 6.5.2.0). Primary outcome measurement was the detection frequency of the predetermined OCT findings in three different OCT scan patterns: 1) volume; 2) six radial scans (R6); and 3) vertical and horizontal radial (R2; extrapolated from the R6 pattern; Figure 1).

OCT examination protocol included R6, through the fovea and a volume scan centered on the fovea. Length of the radial scans was 4 mm. The volume scan had the dimension of  $15^\circ \times 5^\circ$  with the average of minimum 25 A-scans and a distance of  $63\text{ }\mu\text{m}$  between the scans. The OCT scan patterns were examined twice by one observer who was blinded to the clinical information of the patients. Twenty randomly selected cases were examined by an experienced consultant and the intrarater and interrater agreement ratios were analyzed.

**Terminology of the Features** ERM had been characterized as increasing reflectivity on the surface of the retina<sup>[14]</sup>. Epiretinal proliferation is a thick homogenous layer of moderately reflective material between the inner border of the internal limiting membrane and the retinal nerve fiber layer<sup>[15]</sup>. Verticalization was considered as a deep foveal pit<sup>[2]</sup>. Foveoschisis was defined if hyperreflective tissue bridges along wider hyporeflective spaces between the outer nuclear and outer plexiform layers at the fovea<sup>[11]</sup>, which was termed as schitic cavity<sup>[16]</sup>, schitic separation/appearance before<sup>[6]</sup>. Intraretinal cystoid spaces are small, well-circumscribed hyporeflective areas in the inner plexiform layer<sup>[6]</sup>. Irregular foveal contour is the presence of the irregularities of the foveal surface<sup>[2]</sup>. Foveal cavity with undermined edges has recently been described<sup>[11]</sup> as the angle between the retinal surface and

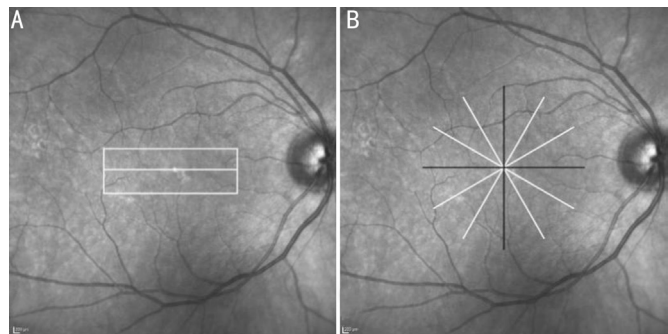


**Figure 1** OCT scan patterns of the right eye A: Volume; B: Six radial scans (R6; 4 white and 2 black lines), and vertical and horizontal radial scans (R2; extrapolated from the R6 pattern (2 black lines).

the edge of the hole less than  $90^\circ$  which was formerly known as a wide, mostly round edged intraretinal, homogeneous, hyporeflective cavitation between the inner and outer retina<sup>[6]</sup>. Ellipsoid line disruption is defined as any interruption or blurring of this line<sup>[11]</sup>, which was formerly named as ellipsoid layer disruption<sup>[6]</sup>.

**Statistical Analysis** Data were analyzed using IBM SPSS Statistics premium 23 V. The kappa statistic was used to test intrarater and interrater reliability. Friedman statistical test was used to detect the features depending on the type of scanning method. Post hoc analysis with Wilcoxon signed-rank tests was conducted with a Bonferroni correction applied, resulting in a significance level set at  $P<0.017$ . The frequency of features detected by three scan patterns was measured by inter quartile range (IQR) and the comparison was made by McNemar's statistical test.

## RESULTS

Of the 100 patients, 66 were female and 34 males. The mean age  $\pm SD$  was  $70.50 \pm 7.33$  y (range 49–89 y). Fifty-five eyes were right and 45 left.

Of the total 8 predetermined features, the maximal detection frequency was found by the volume pattern as  $4.45 \pm 1.45$ . The frequency of the R6 and R2 revealed  $4.35 \pm 1.47$  and  $3.70 \pm 1.59$ , respectively. Regarding the statistical significance of total frequencies, whereas R2 was inferior to the other patterns ( $P<0.001$ ), R6 and volume patterns were comparable ( $P=0.312$ ). The distribution of the feature detection rates based on the OCT scan patterns, and their interquartile values are shown in Table 1.

The statistical evaluation of ERM was not applicable since this feature was detected in almost all eyes by the three different OCT patterns. Statistical analysis showed that R2 was inferior to R6 and volume patterns in detecting foveal cavity with undermined edges and irregular foveal contour, which are criteria for LMH. Epiretinal proliferation and ellipsoid line disruptions, both optional feature for the diagnosis of LMH, were similarly often in all scans patterns. R2 was also inferior

**Table 1 Distribution of the features diagnosed by OCT-scan patterns and interquartile values**

Feature	OCT pattern (n)		
	R2 <sup>a</sup>	R6 <sup>b</sup>	Volume <sup>c</sup>
ERM	99	100	100
Epiretinal proliferation	23	24	23
Verticalization	74	92	94
Foveoschisis	80	90	93
Intraretinal cystoid spaces	34	44	45
Irregular foveal contour	25	39	40
Foveal cavity with undermined edges	22	33	32
Ellipsoid line disruption	10	13	15

OCT: Optical coherence tomography; ERM: Epiretinal membrane;

R2: Vertical and horizontal radial scans; R6: Six radial scans.

<sup>a</sup>Interquartile lower-median-upper values for R2 scan pattern: 3-4-

4.75; <sup>b</sup>Interquartile lower-median-upper values for R6 scan pattern:

3-4-5; <sup>c</sup>Interquartile lower-median-upper values for volume scan

pattern: 3-4-5.75.

**Table 2 Comparison of OCT scan patterns by features (McNemar's statistical test)**

Feature	Comparison of OCT patterns (P-value)		
	R2 vs R6	R2 vs volume	R6 vs volume
ERM	-	-	-
Epiretinal proliferation	1	1	1
Verticalization	<0.001	<0.001	1
Foveoschisis	0.001	<0.001	1
Intraretinal cystoid spaces	0.454	0.031	0.238
Irregular foveal contour	0.001	<0.001	0.774
Foveal cavity with undermined edges	0.006	0.049	1
Ellipsoid line disruption	1	0.375	0.727

OCT: Optical coherence tomography; ERM: Epiretinal membrane;

R2: Vertical and horizontal radial scans; R6: Six radial scans.

in detecting verticalization and intraretinal cystoid spaces, the mandatory features for the diagnoses of MPH. In comparison to R6 and volume, R2 was less sensitive in detecting foveoschisis, which is one mandatory feature for ERM foveoschisis.

In summary, volume and R6 patterns were comparable for epiretinal proliferation, verticalization, foveoschisis and foveal cavity with undermined edges. R2 was inferior to both patterns in revealing verticalization, foveoschisis, irregular foveal contour, and foveal cavity with undermined edges; and additionally, to the volume pattern for intraretinal cystoid spaces (Figures 2-4).

Statistical analysis of the features by different scan patterns is given in Table 2.

Intrarater agreement was in substantial and almost perfect agreement range for the total of 19 evaluations and in moderately agreement range for verticalization and foveoschisis in volume scan analysis. High compliance was found between the two

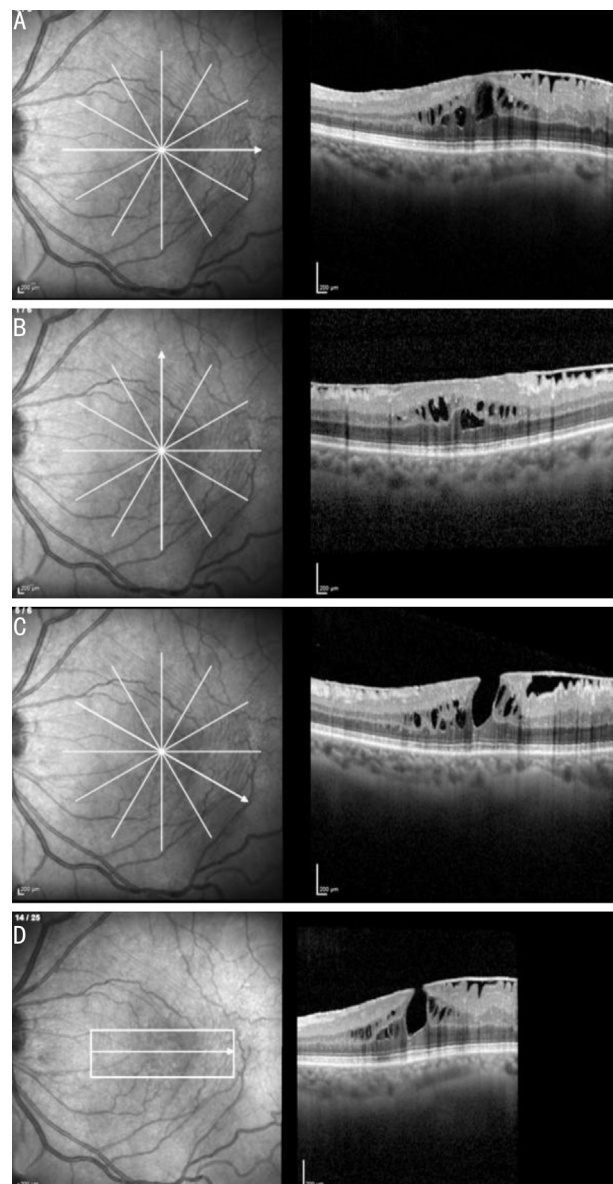


**Figure 2 OCT examination of the left eye** The radial scan is not well-centered due to the ectopy of the fovea. A-B: The horizontal and vertical R2 patterns at macula are showing the epiretinal membrane, thickening of the retina with intraretinal cystoid spaces and schisis, but the verticalization of the fovea is not seen. C-D: The R6 and volume patterns reveal the verticalization in addition to the other features. OCT: Optical coherence tomography; R2: Vertical and horizontal radial scans; R6: Six radial scans.

reviewers in the interrater analysis of OCT scans containing 480 data of 20 patients ( $\text{Kappa value}=0.891\pm0.021$ ).

## DISCUSSION

In the presented study, the detection rate of the morphological features of LMH and MPH were compared by using different OCT-scan patterns. Volume and R6 revealed highest score of predetermined OCT-features, without statistical significant difference between them. The radial scan including only the R2 was inferior to the other two patterns both in the total number and detection of most of the OCT features (Figure 5).

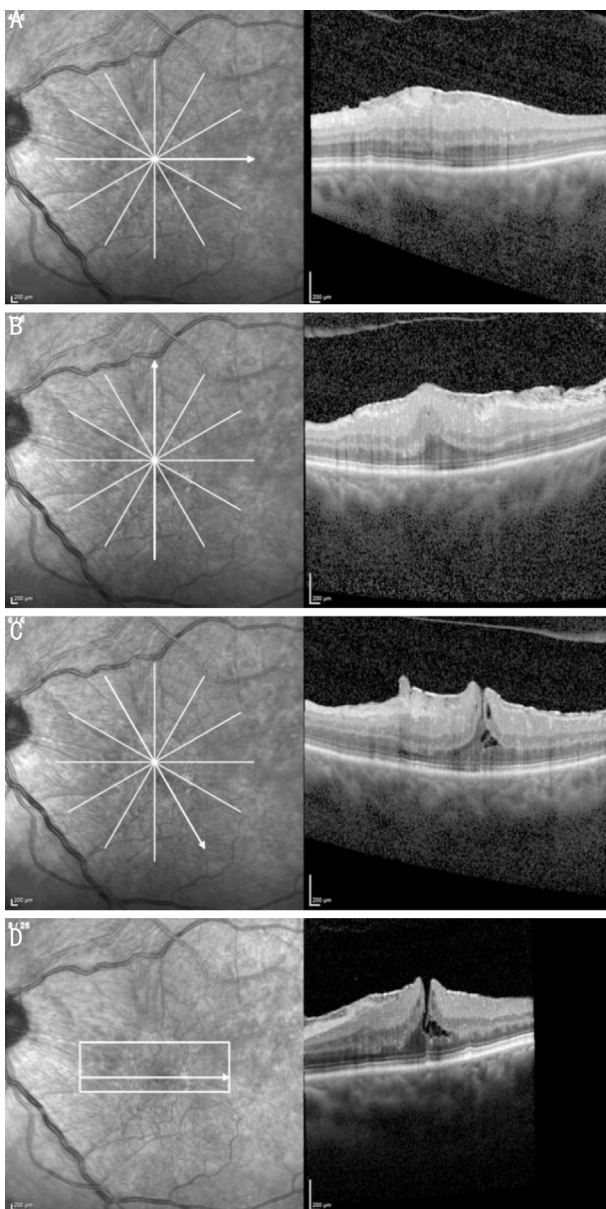


**Figure 3 OCT examination of the left eye** Due to the extreme narrowing of the fovea, the positioning of the radial scan is not optimal. R2 pattern does not show the verticalization, intraretinal cystoid spaces and foveoschisis. A, B: The horizontal and vertical R2 patterns at macula are showing the ERM, thickening of the fovea and loss of the foveal depression. C, D: The R6 and volume patterns are detecting ERM, foveal and parafoveal retinal thickening, intraretinal cystoid spaces, foveoschisis and the verticalization of the fovea. OCT: Optical coherence tomography; ERM: Epiretinal membrane; R2: Vertical and horizontal radial scans; R6: Six radial scans.

Over many decades, the diagnosis of LMH and MPH was based on ophthalmoscopy and fundus photography<sup>[17-18]</sup>. In the 90s, OCT examination became the method of choice in management of the vitreomacular interface diseases<sup>[16,19]</sup>. Consequently, the definition of vitreomacular interface diseases were adapted to the features obtained by the OCT. The continuous improvement of OCT imaging has contributed to an increase in knowledge and modification

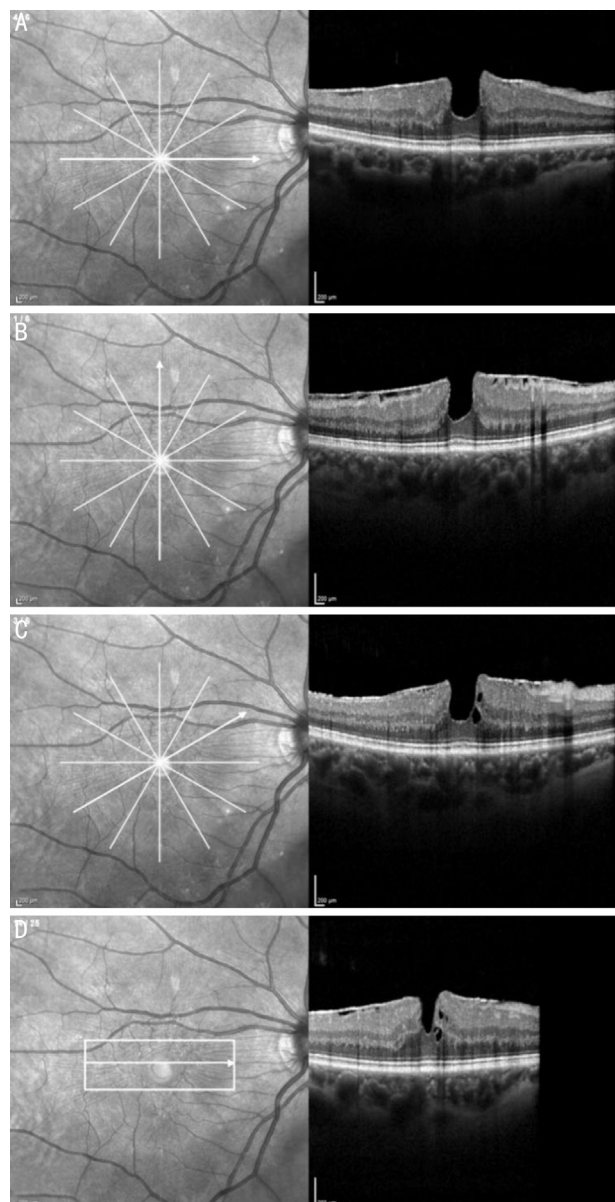


**Figure 4 OCT examination of the right eye** The radial scan is well-centered. The intraretinal cystoid spaces and foveoschisis are limited to the supero-nasal edge of the fovea, and therefore not covered by the R2 pattern, even perfectly positioned. A, B: The horizontal and vertical R2 patterns through the foveal center are showing the ERM, parafoveal thickening of the retina and verticalization. C, D: The R6 and volume patterns are detecting additionally the intraretinal cystoid spaces and foveoschisis at the supero-nasal edge of the fovea. OCT: Optical coherence tomography; R2: Vertical and horizontal radial scans; R6: Six radial scans.

or revisions of the definitions<sup>[7-11]</sup>. Another important issue has been the inconsistencies between the interraters in the diagnosis of the vitreomacular interface diseases. A study evaluated the effect of the nomenclature of the vitreomacular interface diseases and reported that the International Vitreomacular Traction Study (IVTS) classification leads to higher rates of accuracy in diagnosing vitreomacular interface diseases<sup>[20]</sup>.

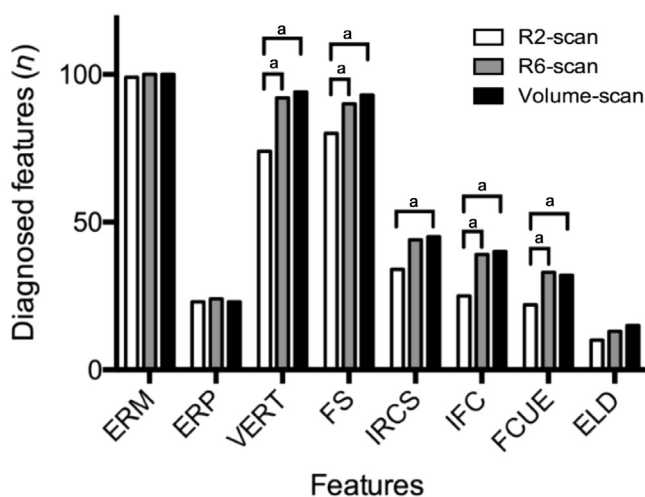


**Figure 5 Comparison of the different scan patterns with regard to the diagnosed OCT features** ERM: Epiretinal membrane; ERP: Epiretinal proliferation; VERT: Verticalization; FS: Foveoschisis; IRCS: Intraretinal cystoid spaces; IFC: Irregular foveal contour; FCUE: Foveal cavity with undermined edges; ELD: Ellipsoid line disruption.  $^aP<0.05$ .

In a recently published consensus manuscript, the OCT criteria of the LMH and MPH were redefined<sup>[11]</sup>. The diagnosis of the LMH was based on three mandatory criteria: irregular foveal contour, foveal cavity with undermined edges and the apparent loss of foveal tissue. Optional anatomical features included three criteria: the presence of epiretinal proliferation, the presence of a central foveal bump and the disruption of the ellipsoid zone. The MPH diagnosis was based on three mandatory criteria: foveal sparing ERM, steepened (verticalized) foveal profile and an increased central retinal thickness. Optional anatomical features were the presence of microcystoid spaces in the inner nuclear layer and a normal retinal thickness<sup>[11]</sup>.

Not only were the definitions of the certain vitreomacular interface diseases a subject for change. The applied technique in OCT examination for the macular morphology was also evaluated. It was reported that high-density radial scanning demonstrated superior detection rates of small full-thickness macular holes compared to standard raster volume scanning and standard radial scanning<sup>[12]</sup>. In another article, the 6-line radial scan was statistically inferior to the 25-line raster at detecting fluid in neovascular age-related macular degeneration, but superior at detecting early macular hole formation and demonstrating a positive trend in identifying focal vitreomacular traction<sup>[13]</sup>.

In our study, the statistical analysis showed comparable results of the R6 and volume patterns in determining the total number and of each selected OCT features. R2 was inferior to the other OCT scan patterns. Features such as epiretinal proliferation and ellipsoid line disruptions were detected equally using

the three patterns. The frequency of the foveal cavity with undermined edges was seen as 33%, 32%, and 22% by R6, volume, and R2, respectively. Both of R6 and volume patterns were statistically superior to R2.

The pathological dynamics in the vitreomacular interface diseases may show a wide heterogeneity which challenges a precise diagnosis. As example, the morphological changes in the fovea may not necessarily begin symmetrical in and around the foveal edge. And features thought characterizing different clinical entities, for example foveal cavity with undermined edge and verticalization may exist in the same eye at the same time. Therefore, a comprehensive evaluation of the fovea by a standard OCT-protocol may increase the chance of the detection of all clinically significant features and allows a precise diagnosis.

Our study has some limitations. It is retrospective and based on one center. Because of the low incidence of the pseudo-operculum on the OCT-examination and possible intra- and interrater measurement differences of the retinal thickness, we did not include these features into our analysis. Since these features are mandatory criteria for the diagnosis of LMH, the presented study, by design, does not provide a direct comparison of the OCT scan patterns for the diagnosis of LMH but rather a comparison of some predetermined features. On the other hand, eyes with the commonest features seen in LMH and MPH were analyzed by using the available OCT examination performed in the daily routine. Although randomly selected in a series of 100 cases, evaluation of only 20 patients for interrater reliability can be considered as a limitation. We not only took the diagnostic criteria as reference in the diagnosis of LMH and MPH<sup>[11]</sup>, but also examined some other OCT entities to facilitate a comparison with other similar studies. One may assume that in some patients with eccentric fixation, the probability of catching a foveal lesion in R2 pattern is already low, a possible cause of bias. Manual foveal fixation corrections were not taken into account, if any, in eyes with eccentric fixation since the study was addressed to anatomical fovea. On the other hand, since patients are advised to look inside the aiming beam, this source of error, if any, should be minimal. Another point is that the volume pattern, considering an area of fovea-centred  $15^\circ \times 5^\circ$  may not cover additional perifoveal pathologies.

In summary, we evaluated the advantages and limits of different OCT scan patterns in the identification of morphological features seen in LMH and MPH in real world conditions. The R6 and volume scans of the OCT showed comparable results in morphological features detection, whereas the R2 was found inferior to the other patterns. The physician should be aware that the selection of OCT-scan patterns may influence the detection of mandatory features to

establish the diagnosis of LMH and MPH. The combination of different OCT scan patterns may likely increase the detection frequency of the relevant features and improve the diagnostic accuracy.

## ACKNOWLEDGEMENTS

Special thanks to Sarp Uner (MD, Lokman Hekim University, Medical School, Department of Public Health) for statistical analysis and critical review.

**Authors' contributions:** Conceptualization: Uyar OM, Neubauer J; data collection and curation: Uyar OM, Gelisken F, Neubauer J, Sadler F, Konrad EM; draft preparation: Uyar OM, Gelisken F; revision and editing: Uyar OM, Gelisken F, Neubauer J, Sadler F, Konrad EM.

**Conflicts of Interest:** **Uyar OM**, None; **Neubauer J**, None; **Sadler F**, None; **Konrad EM**, None; **Gelisken F**, None.

## REFERENCES

- 1 Gaudric A, Haouchine B, Massin P, Paques M, Blain P, Erginay A. Macular hole formation: new data provided by optical coherence tomography. *Arch Ophthalmol* 1999;117(6):744-751.
- 2 Haouchine B, Massin P, Tadayoni R, Erginay A, Gaudric A. Diagnosis of macular pseudoholes and lamellar macular holes by optical coherence tomography. *Am J Ophthalmol* 2004;138(5):732-739.
- 3 Witkin AJ, Ko TH, Fujimoto JG, Schuman JS, Baumal CR, Rogers AH, Reichel E, Duker JS. Redefining lamellar holes and the vitreomacular interface: an ultrahigh-resolution optical coherence tomography study. *Ophthalmology* 2006;113(3):388-397.
- 4 Androudi S, Stangos A, Brazitikos PD. Lamellar macular holes: tomographic features and surgical outcome. *Am J Ophthalmol* 2009;148(3):420-426.
- 5 Zampedri E, Romanelli F, Semeraro F, Parolini B, Frisina R. Spectral-domain optical coherence tomography findings in idiopathic lamellar macular hole. *Graefes Arch Clin Exp Ophthalmol* 2017;255(4):699-707.
- 6 Govetto A, Dacquay Y, Farajzadeh M, Platner E, Hirabayashi K, Hosseini H, Schwartz SD, Hubschman JP. Lamellar macular hole: two distinct clinical entities? *Am J Ophthalmol* 2016;164:99-109.
- 7 Staurenghi G, Sadda S, Chakravarthy U, Spaide RF, International Nomenclature for Optical Coherence Tomography (IN•OCT) Panel. Proposed lexicon for anatomic landmarks in normal posterior segment spectral-domain optical coherence tomography: the IN•OCT consensus. *Ophthalmology* 2014;121(8):1572-1578.
- 8 Duker JS, Kaiser PK, Binder S, de Smet MD, Gaudric A, Reichel E, Sadda SR, Sebag J, Spaide RF, Stalmans P. The international vitreomacular traction study group classification of vitreomacular adhesion, traction, and macular hole. *Ophthalmology* 2013;120(12):2611-2619.
- 9 Spaide RF, Curcio CA. Anatomical correlates to the bands seen in the outer retina by optical coherence tomography: literature review and model. *Retina* 2011;31(8):1609-1619.
- 10 Gattoussi S, Buitendijk GHS, Peto T, Leung I, Schmitz-Valckenberg S, Oishi A, Wolf S, Deák G, Delcourt C, Klaver CCW, Korobelnik JF, Consortium EEE. The European Eye Epidemiology spectral-domain optical coherence tomography classification of macular diseases for epidemiological studies. *Acta Ophthalmol* 2019;97(4):364-371.
- 11 Hubschman JP, Govetto A, Spaide RF, Schumann R, Steel D, Figueroa MS, Sebag J, Gaudric A, Staurenghi G, Haritoglou C, Kadonosono K, Thompson JT, Chang S, Bottoni F, Tadayoni R. Optical coherence tomography-based consensus definition for lamellar macular hole. *Br J Ophthalmol* 2020;104(12):1741-1747.
- 12 Schneider EW, Todorich B, Kelly MP, Mahmoud TH. Effect of optical coherence tomography scan pattern and density on the detection of full-thickness macular holes. *Am J Ophthalmol* 2014;157(5):978-984.
- 13 Rahimy E, Rayess N, Maguire JI, Hsu J. Radial versus raster spectral-domain optical coherence tomography scan patterns for detection of macular pathology. *Am J Ophthalmol* 2014;158(2):345-353.e2.
- 14 Wickham L, Gregor Z. Epiretinal membranes. In *Retina textbook*, SJ Ryan, 5th edn., Mosby (Maryland, US) 2013;116:1958.
- 15 Pang CE, Spaide RF, Freund KB. Epiretinal proliferation seen in association with lamellar macular holes: a distinct clinical entity. *Retina* 2014;34(8):1513-1523.
- 16 Wilkins JR, Puliafito CA, Hee MR, Duker JS, Reichel E, Coker JG, Schuman JS, Swanson EA, Fujimoto JG. Characterization of epiretinal membranes using optical coherence tomography. *Ophthalmology* 1996;103(12):2142-2151.
- 17 Allen AW Jr, Gass JD. Contraction of a perifoveal epiretinal membrane simulating a macular hole. *Am J Ophthalmol* 1976;82(5):684-691.
- 18 Gass JD. Lamellar macular hole: a complication of cystoid macular edema after cataract extraction. *Arch Ophthalmol* 1976;94(5):793-800.
- 19 Puliafito CA, Hee MR, Lin CP, Reichel E, Schuman JS, Duker JS, Izatt JA, Swanson EA, Fujimoto JG. Imaging of macular diseases with optical coherence tomography. *Ophthalmology* 1995;102(2):217-229.
- 20 Benyamin S, Loewenstein A, Moisseiev E. Evaluation of accuracy and uniformity of the nomenclature of vitreoretinal interface disorders. *Retina* 2020;40(7):1272-1278.